Integrating 3D Modelling and Non-linear Numerical Simulations in Concrete Additive Manufacturing

Jiri Rymes[1[0000-0003-3288-0826]], Jan Cervenka[1[0000-0003-4945-1163]], Libor Jendele[1[N/A]], Vladislav Bures[2[N/A]], David Citek[3[0000-0002-2615-1873]]

[1] Cervenka Consulting s.r.o., Prague, Czech Rep.
[2] Technical University of Liberec, Liberec, Czech Rep.
[3] Klokner Institute, Prague, Czech Rep.
jiri.rymes@cervenka.cz

Additive manufacturing is an emerging technology that is gradually being adopted in the construction industry. When assessing the structural integrity of elements built using 3D concrete printing, careful consideration is required for unique structural aspects like a potentially weaker interlayer bond or geometric imperfections arising from the printing process. This study addressed these aspects by the means of non-linear finite element method. A single comprehensive analysis covering the entire lifecycle of a 3D-printed element from the construction process until a final load test is presented. First in the analysis, the printing process is simulated to check the stability of the element during manufacturing. The deformation from the early age is kept in the model and subsequently automatically considered during the load test simulation. The outcomes of the load test simulation are compared with experimental results for validation.

Keywords: Additive manufacturing (AM), 3D Concrete Printing (3DCP), Finite Element Analysis, Non-linear Analysis, Early-age Material Properties, Load-bearing capacity

1 Introduction

3D Concrete Printing (3DCP) is a rapidly emerging technology transforming the concrete industry and construction sector in general. It allows automatization of the construction process while enabling the building of architectural designs previously impossible with traditional methods. Compared to the site-cast or precast concrete technologies, specific aspects need to be addressed in the field of additive manufacturing. While concrete material can be generally regarded as an isotropic medium on the macroscopic scale, the layer-by-layer construction method introduces inhomogeneity into the material. The bond between two layers has generally lower mechanical performance characteristics compared to the rest of the bulk material [1]. This is typical for the additive technology where fresh paste is deposited on top of the previously printed material and their connection relies on the ability of the material to bond. Furthermore, in the case of fiber reinforced concrete mixtures, the microfibers are present only in the printed layer but do not cross between two layers. The interlayer connection thus represents a possible weak spot in the printed element.

The next specific aspect of elements constructed by 3DCP is the geometrical imperfections. The imperfections can originate either from imprecise deposition of the paste or deformation of the element in its fresh state. As further layers are printed, the weight transferred by the bottom layers increases. At this

stage, their mechanical performance characteristics are governed by the viscous, thixotropic nature of the fresh paste. The low material stiffness may lead to increasing deformation and even buckling of the printed element [2]. Any excessive deformation during manufacturing may later significantly affect the mechanical behaviour of the structure in the mature age.

Both interlayer bonds and possible early-age deformation affect the mechanical behaviour of the printed element and its load-bearing capacity in the mature age. The non-linear finite elements method (FEM) has the potential to offer insight into the behaviour of 3DCP elements. When non-linear relations are implemented in the material model, a realistic structural response can be obtained from the simulations. In the field of 3DCP, it has been shown that non-linear FEM analysis can reproduce the buckling collapse mechanism observed during printing in laboratory conditions [3]. A similar approach was used for the simulation of a real house structure [4]. For these analyses, a time-dependent material model was developed allowing adjustment of the material parameters during the analysis run thus simulating the hardening of the fresh paste. The hardening of the material can be captured by relating the underlying hydration process and the concrete compressive strength, which can be further used to deduce the remaining material parameters required for FEM analysis [4].

In the study presented here, we show a complex analysis aiming at determining the maximum load-bearing capacity of the actual 3D-printed element. The analysis is composed of three intervals. First, the printed phase is simulated to assess the stability of the structure during construction. Next, the maturing phase is simulated when the material gains strength while subjected to shrinkage. Finally, a compression test is simulated to determine the element's strength. Since the entire history is simulated within a single analysis, the deformation from the printing phase is kept in the model and enters the simulation of the loading test as an initial imperfection.

2 Experimental and Numerical Methods

2.1 3D-printed Wall Segment

As part of the experimental program, a 3DCP wall segment with base dimensions of 300 × 970 mm and height of 800 mm was prepared at the Klokner Institute, Prague, Czech Republic. The width of the printed layer was 20 mm. Along the longer edge, the wall segment was stiffened by inner stiffeners for better overall mechanical performance. The compressive strength of the material used for printing is 50 MPa at 28 days. A photo of the element after the printing is shown in **Fig. 1**. After maturing, the wall segment was subjected to compressive strength to determine its load-bearing capacity.

Fig. 1 Photo of the 3D-printed wall segment.

2.2 Finite Element Model

A finite element model was developed to reproduce the results of the experimental program. The model of the wall segment consisted of 27 680 elements with quadratic approximation, each having 3 degrees of freedom. The mesh of the wall segment is shown in **Fig. 2** (a). To capture the anisotropy in the structure due to 3DCP, horizontal interface elements were modelled between every layer. Furthermore, a vertical interface was modelled inside of the two inner stiffeners. The geometry of the interfaces is shown in **Fig. 2** (b) together with the loading plate modelled for the application of the vertical displacement during the load test simulation.

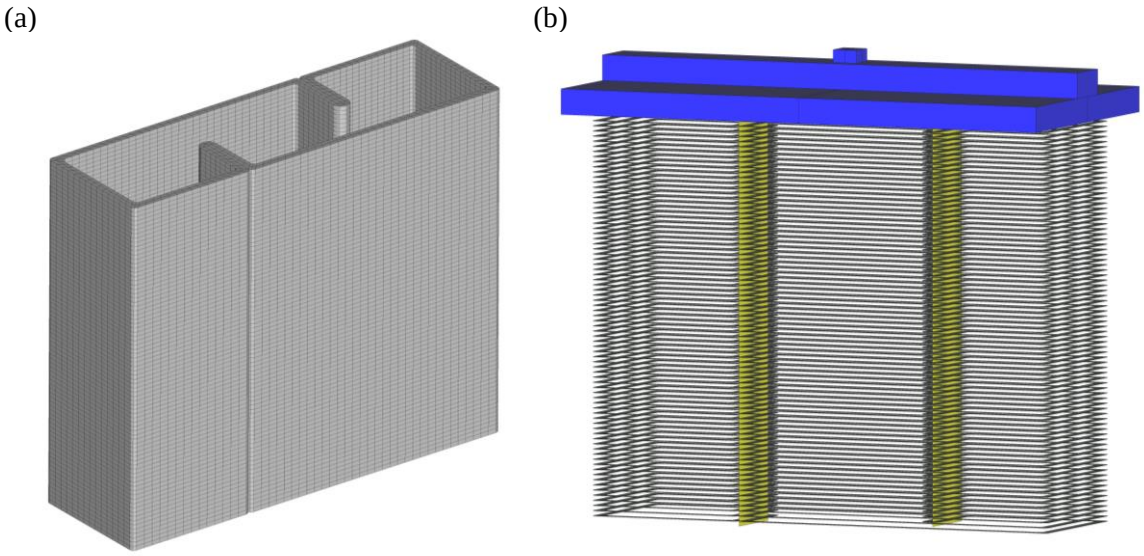

Fig. 2 Numerical model of the wall segment: (a) Finite element mesh of the concrete elements and (b) Geometry of the horizontal (i.e., interlayer) and vertical interfaces together with the geometry of the loading plate.

2.3 Simulation of Construction Process

In non-linear FEM, loads are typically incrementally applied in multiple solutions steps. For additive manufacturing simulations, each load step can represent a specific time during the construction. Before the solution starts, each element in the model is assigned a specific construction time. The construction time corresponds to the actual time when a specific part of the structure gets printed in reality and is determined by the printing nozzle's trajectory and speed. In the study presented here, the speed of the nozzle was assumed as 120 mm/s. During the solution, the finite elements are progressively activated along the printing trajectory based on their construction time.

Once activated, the finite element is loaded with the body load equal to the self-weight of the material. Therefore, the total self-weight in the model corresponds only to the body load of the already-activated elements. A similar approach is utilized for shrinkage loads where the construction time governs the gradual application of initial strain. This results in differential shrinkage along the model.

The analysis method uses the updated Lagrangian formulation which updates the nodal coordinates after each solution step based on the calculated deformation. This allows for capturing the gradual deformation of the model during printing and the second-order effects during the simulation of the loading experiment.

2.4 Material Model

The material model used for the simulation is an extension of the fracture-plastic model of Červenka et al. [1, 6]. The model decomposes the mechanical response in tension and compression. When the maximum tensile strength of the material is exceeded, crack formation is simulated using the smeared crack

model with a crack band. The crack opening law is based on the fracture energy approach considering the amount of the dissipated energy in the fracture process. In compression, the Menetrey & Willam [7] failure criterion is adopted with linear softening limited by the maximum compressive displacement. This combined approach adopted in the material model allows for obtaining realistic material response at ultimate stress both in tension and compression. Further information about the material model can be found in our other publications, such as [8 – 10].

The basic fracture-plastic model was extended with a kinetic part allowing simulation of the gradual evolution of the material parameters during the simulation run and thus simulating hardening of the printed concrete paste. In each solution step, a group of finite elements is activated according to the printing speed and trajectory. The element construction time corresponds to the element activation and is further used to determine the current material parameters at each step. Ideally, a single material model should be capable of covering the entire material history thus allowing complex assessment of the structural integrity, both during the 3DCP process and at maturity. In the fresh state, the concrete paste behaves as a non-Newtonian fluid and its material performance originates from its thixotropic characteristics [11]. During printing, the applied external stress disturbs inter-particle bonds in the paste allowing deposition of the paste. After printing inter-particle bonds are re-created leading to an increase in the yield stress. This stage is followed by the structuration phase when the nature of the material starts to harden [11, 12]. Finally, further hardening of the paste is governed by the hydration process similar to the maturing of conventional concrete. If the material model used in the simulation captures the changing nature of the fresh paste to hardened concrete, a single analysis can cover the entire lifecycle of the 3DCP element. The deformation occurring during printing enters the simulation of the loading test as the initial imperfection and thus is accounted for.

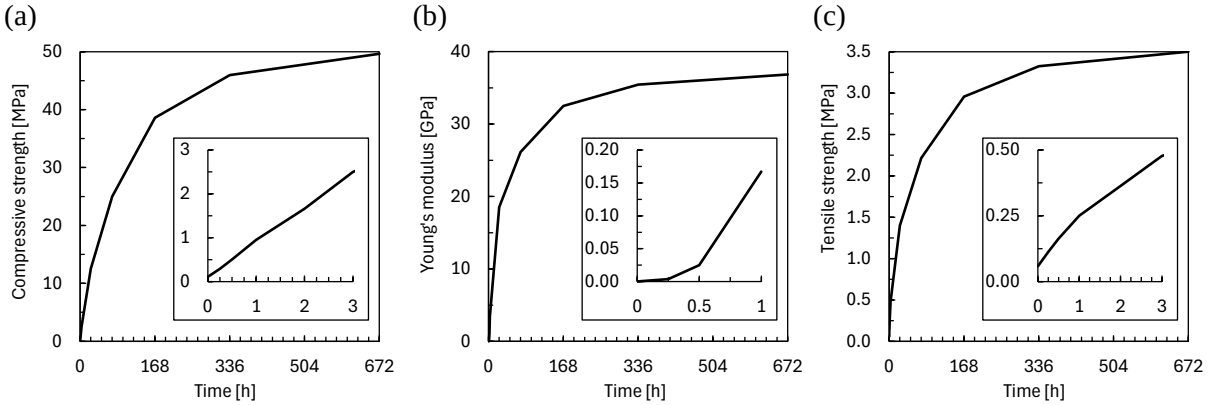

Fig. 3 Development of the mechanical properties of the fresh concrete material: (a) Compressive strength, (b) Young's modulus, and (c) Tensile strength. The details show the development at an early age.

The development of the compressive strength was based on the experimental data which were available from the material age of 15 minutes. The values of time development of the Young's modulus, which are important for the deformation during printing were not available for the young material therefore they were assumed to develop exponentially between age 0 min and the measured values at the age of 2 and 3 hours. The initial value of Young's modulus at time 0 min was taken as 0.153 MPa same as for the material presented in the study of Esposito et al. [13]. The evolution of the compressive strength, Young's modulus, and tensile strength in time are plotted in **Fig. 3**. The remaining parameters of the material model were deduced from the evolution of the compressive strength using the formulas summarised in **Table 1**. These relations are slight modifications of those given in [4].

The Mohr-Coloumb material model was used for the interlayer interfaces and vertical interfaces in the inner stiffeners shown in **Fig. 2** (b). Their material parameters are given in

Table 2. The adopted Mohr-Coloumb interface model allows the opening of the interface once its tensile strength is exceeded as well as shear sliding.

Table 1 Relations used for generation of the parameters of the fracture-plastic material model based on the compressive strength $f_c(t)$.

Parameter: symbol [unit]	Formula
Young's modulus: E [MPa]	$0.153 + 0.00208t^{2.757}$ if t < 1×24×60 min $\left(6000 - 15.5 f_{c,28}\right)\sqrt{f_c(t)}$ if $t \geq$ 1×24×60 min
Tensile strength: f_t [MPa]	$3.5[f_c(t) / f_{c,28}]^{\frac{2}{3}}$
Specific fracture energy: G_f [N/m]	$73 f_c(t)^{0.18}$
Critical compressive displacement: w_d [mm]	- 0.25
Onset of non-linearity in compression: f_{c0} [MPa]	$f_c(t)/3$
Plastic strain at compressive strength: ε_{cp} [-]	$f_c(t) / E_{28}$

Table 2.Material parameters of the interfaces used in the numerical model.

Parameter: symbol [unit]	Horizontal interface (interlayer)	Vertical interface (in the inner stiffener)
Tensile strength: $f_{t,int}$ [MPa]	0.50	0.25
Cohesion: c [MPa]	0.50	0.25
Friction coefficient: μ [-]	0.5	0.5

3 Results and Discussion

The displacement showing a gradual buckling of the printed element is shown in **Fig. 4** for 15, 25, and 30 minutes of the printing process. From the numerical results, the maximum out-of-plane deformation at the end of the printing process reached 5.5 mm in the longer portion of the longitudinal wall. This deformation enters the simulation of the compression test as an initial imperfection.

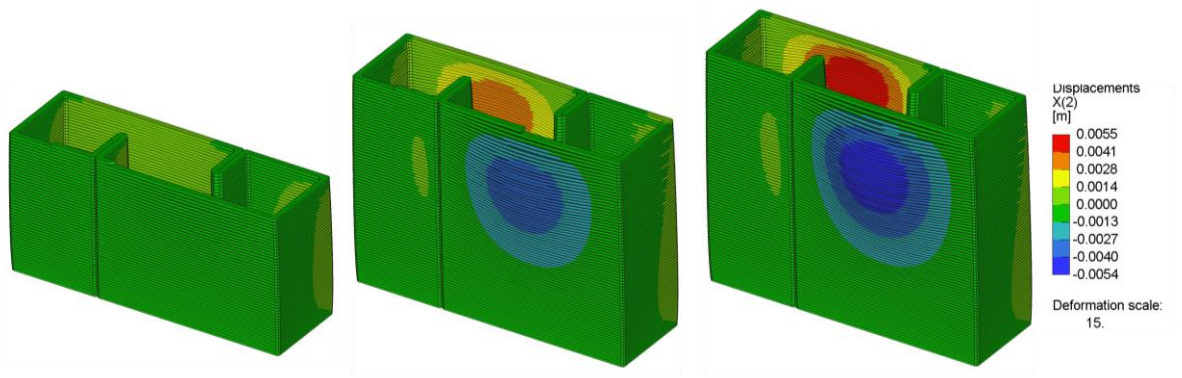

Fig. 4 Out-of-plane displacement perpendicular to the longitudinal dimension of the wall showing gradual buckling at: (a) 15 minutes, (b) 25 minutes, and (c) at the end of printing at 30 minutes (deformation scale ×15).

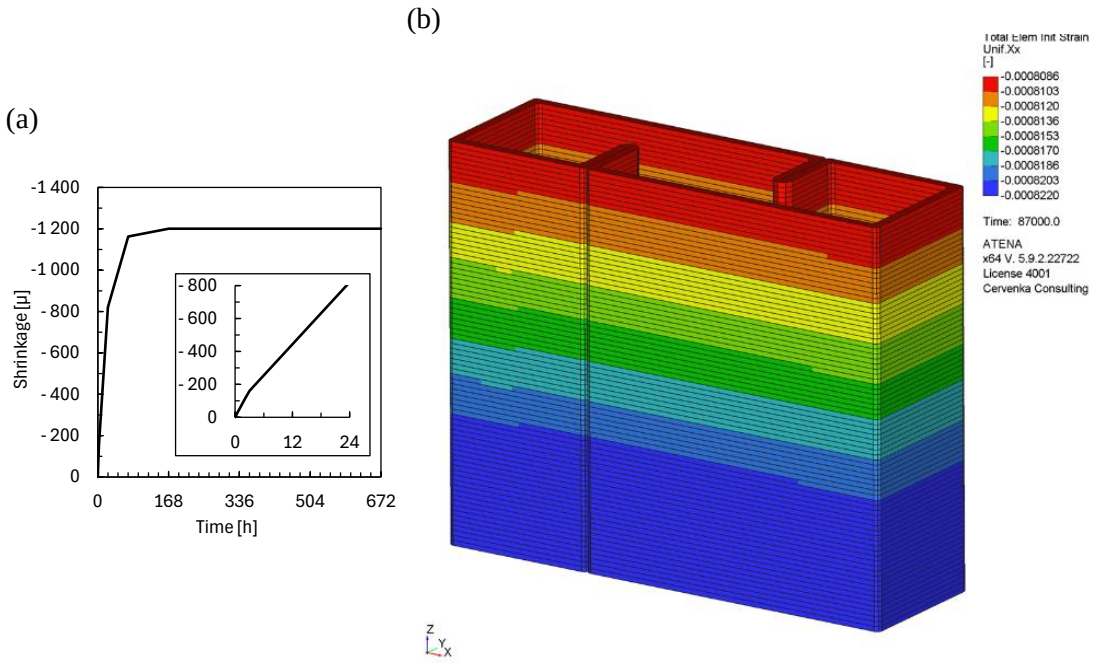

Fig. 5 Shrinkage load applied on the model: (a) Shrinkage evolution in time and (b) Differential shrinkage strain on the model at the time of 1 day.

In the simulation, the shrinkage strain of -1200 μ was applied to the model in the form of initial strain. The evolution of the shrinkage used in the analysis is plotted in **Fig. 5** (a) and the distribution of the initial strain in the model is shown in **Fig. 5** (b) at the time of 1 day. The shrinkage load did not result in any crack formation in the simulation.

A loading test was simulated at the age of 28 days. **Fig. 6** shows a comparison between the load-displacement diagram measured in the experiment and the analysis results. It shows a good agreement both in the peak load and stiffness. The maximum load measured in the experiment was 818 kN while the model predicted failure at 764 kN. For comparison, another analysis that neglected the interlayer and vertical interfaces as well as the construction processes was conducted. This analysis gave the maximum loading capacity of 2044 kN. Therefore, neglecting the weaker interlayer bond and imperfection from the printing process resulted in an overestimation of the actual load-bearing capacity by 168 %.

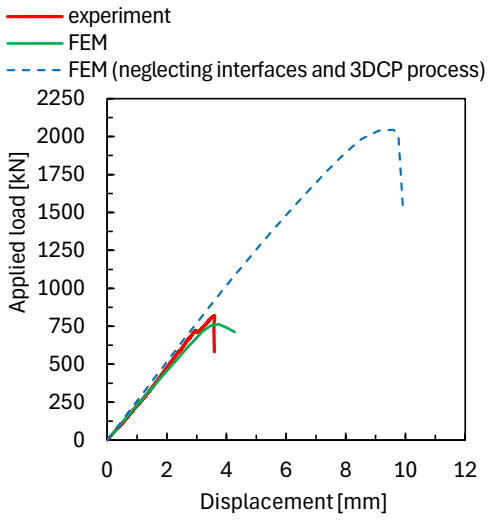

Fig. 6 Comparison of the load-displacement diagram from the experiment and analyses. The blue dashed curve shows analysis results neglecting interfaces and the simulation of the printing process thus having no initial imperfection.

(a) (b)

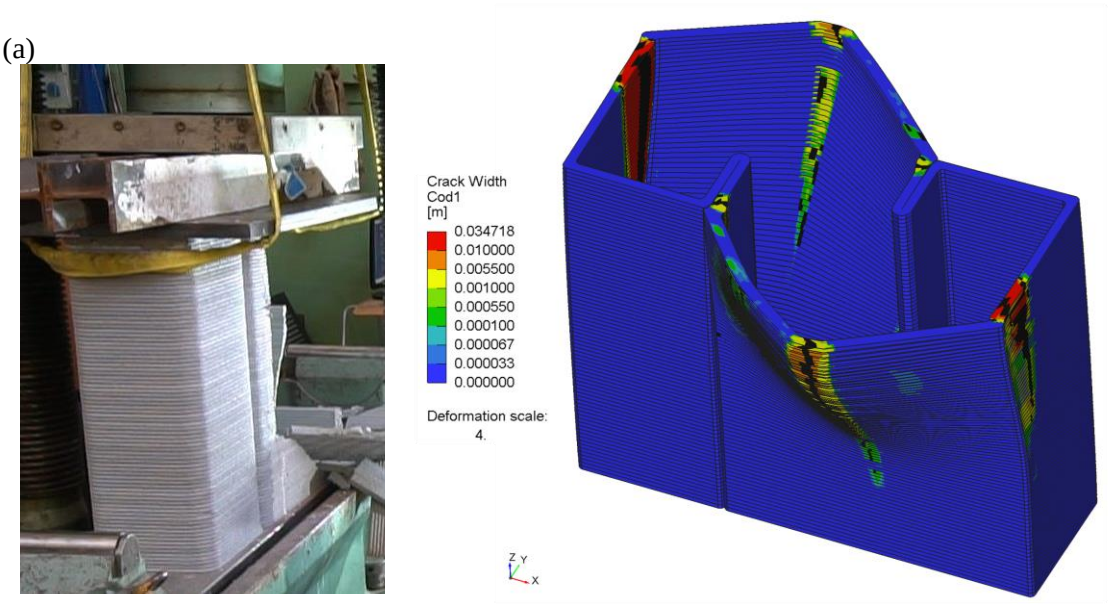

Fig. 7 Post-peak failure mode: (a) Experimental results, and (b) Crack width in the numerical results (deformation scale ×4, only cracks larger than 0.1 mm are emphasised).

The simulation results showed a similar failure mechanism as in the experiment. As the load increases, the horizontal deformation in the longer portion of the longitudinal wall increases. This is associated with crack formation at both ends of this wall portion and at its center. Finally, at the peak load, this part of the element undergoes out-of-plane brittle collapse. The failure modes observed in the experiment and in the numerical analysis is shown in **Fig. 7**. For comparison, the failure model observed in the analysis neglecting the interfaces and the simulation of the 3DCP process is plotted in **Fig. 8**.

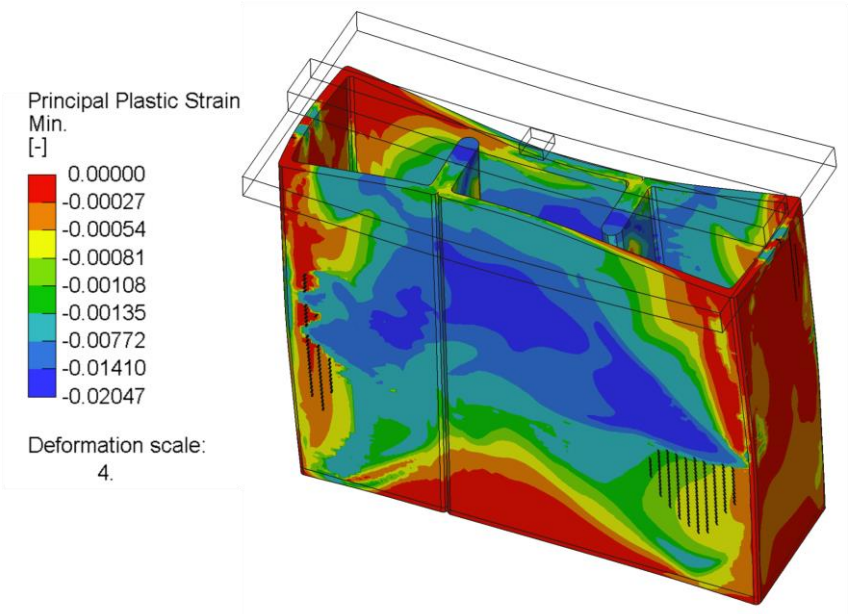

Fig. 8 Post-peak failure mode in the model neglecting interfaces and the simulation of the 3DCP process (deformation scale ×4, only cracks larger than 0.1 mm are emphasised).

4 Conclusions

This study presents a complex non-linear FEM analysis assessing the structural behaviour of a 3DCP element, both at the early and mature age. The analysis relies on a time-dependent material model allowing for simulating the change in the nature of the material from the fresh paste to the hardened concrete. First, the concrete printing process was simulated through the gradual activation of the finite elements along the printing trajectory. This allowed assessment of the stability during construction. Weaker interlayer bonds between the printed layers were captured through interface elements within the model. The calculated deformation in the early age was kept in the model and influenced the structural performance during the load test simulation in the mature age. By comparing the load-displacement curves and failure modes obtained from the analysis and experiment, the ability of the FEM model to reproduce actual mechanical behaviour was validated.

The numerical model was further used to calculate the idealised maximum load-bearing capacity of the element when assuming a perfect interlayer bond and no initial imperfection. The analysis suggested that, in the particular case of this element, neglecting these important aspects of the 3DCP structure may lead to an overestimation of the actual load-bearing capacity by 168 %.

These findings highlight the critical importance of considering the unique characteristics of additively manufactured elements for accurate load-bearing capacity assessments. Furthermore, the potential of non-linear FEM for comprehensive evaluations of the structural integrity of 3DDCP elements from the early to mature age.

Acknowledgement

This work was supported by the Czech Technology Agency and Ministry of Industry and Commerce under the program TREND and project no. FW06010422 “Simulation and design of structures from digital concrete”. The financial support is greatly acknowledged.

References

1. Keita E., Bessaies-Bey H., Zuo W., Belin P. & Roussel N. (2019). Weak bond strength between successive layers in extrusion-based additive manufacturing: measurement and physical origin. Cement and Concrete Research, 123, 105787.
2. Wolfs R. J. M., Bos F. P. & Salet T. A. M. (2018). Early Age Mechanical Behaviour of 3D Printed Concrete: Numerical Modelling and Experimental Testing Cement and Concrete Research, 106, pp 103-116.
3. Vaitová M., Jendele L. & Červenka J. (2020) Printing of Concrete Structures Modelled by FEM, Solid State Phenom. 309, pp 261–266.
4. Rymeš J., Červenka J. & Jendele L. (2023) Material Modelling and Simulation of 3D Concrete Printing Process. Proceedings of FraMCoS-11.
5. Červenka J., Červenka V. & Eligehausen R. (1998). Fracture-plastic material model for concrete, application to analysis of powder actuated anchors. In: Proceedings FRAMCOS (3). pp 1107–1116.
6. Červenka J. & Papanikolaou V.K. (2008). Three-dimensional combined fracture–plastic material model for concrete. Int J Plast 24, pp 2192–2220.
7. Menetrey P. & Willam K. J. (1995). Triaxial failure criterion for concrete and its generalization. Structural Journal, 92(3), pp 311-318.
8. Červenka V., Červenka, J. & Jendele, L. (2023). ATENA Program Documentation, Part 1: Theory, 2023, Cervenka Consulting s.r.o., www.cervenka.cz
9. Červenka V., Červenka J., Kadlec L. (2018). Model uncertainties in numerical simulations of reinforced concrete structures. Struct Concr. 19(6), pp 2004–2016.
10. Červenka, V., Červenka J., & Rymeš J. (2024). Numerical simulation of concrete structures—From research to engineering application. Structural Concrete.
11. Roussel N. (2006). A thixotropy model for fresh fluid concretes: Theory, validation and applications, Cem. Concr. Res. 36, pp 1797–1806.
12. Kruger J., Zeranka S. & van Zijl G. (2019). An ab initio approach for thixotropy characterisation of (nanoparticle-infused) 3D printable concrete, Constr. Build. Mater. 224, pp 372–386.
13. Esposito L., Casagrande L., Menna C., Asprone, D. & Auricchio F. (2021). Early-age creep behaviour of 3D printable mortars: experimental characterisation and analytical modelling. Materials and Structures, 54, pp 1-16.